

**LA-UR-23-21163**

Accepted Manuscript

## **Analysis of Coronado State Historic Site artifacts using X-rays**

Young, Steven Glen  
Valdez, James Anthony  
Espy, Michelle A.  
Edgar, Alexander Steven  
Brett, Jack Kevin  
Pettes, Michael Thompson  
Mathers, Clay  
Barbour, Matthew  
Patterson, Brian M.

Provided by the author(s) and the Los Alamos National Laboratory (2024-07-02).

**To be published in:** X-Ray Spectrometry

**DOI to publisher's version:** 10.1002/xrs.3350

**Permalink to record:**



<https://permalink.lanl.gov/object/view?what=info:lanl-repo/lareport/LA-UR-23-21163>



Los Alamos National Laboratory, an affirmative action/equal opportunity employer, is operated by Triad National Security, LLC for the National Nuclear Security Administration of U.S. Department of Energy under contract 89233218CNA000001. By approving this article, the publisher recognizes that the U.S. Government retains nonexclusive, royalty-free license to publish or reproduce the published form of this contribution, or to allow others to do so, for U.S. Government purposes. Los Alamos National Laboratory requests that the publisher identify this article as work performed under the auspices of the U.S. Department of Energy. Los Alamos National Laboratory strongly supports academic freedom and a researcher's right to publish; as an institution, however, the Laboratory does not endorse the viewpoint of a publication or guarantee its technical correctness.

## RESEARCH ARTICLE

# Analysis of Coronado State Historic Site artifacts using X-rays

Steven G. Young<sup>1</sup> | James Valdez<sup>2</sup> | Michelle Espy<sup>3</sup> | Alex Edgar<sup>1</sup>  |  
Jack Brett<sup>1</sup> | Michael T. Pettes<sup>4</sup> | Clay Mathers<sup>5</sup> | Matthew Barbour<sup>6</sup> |  
Brian M. Patterson<sup>1</sup> 

<sup>1</sup>Engineered Materials Group, Materials Science and Technology Division, Los Alamos National Laboratory, Los Alamos, New Mexico, USA

<sup>2</sup>Materials Science in Radiation and Dynamics Extremes Group, Materials Science and Technology Division, Los Alamos National Laboratory, Los Alamos, New Mexico, USA

<sup>3</sup>Non-destructive Testing and Evaluation Group, Engineering Technology and Design Division, Los Alamos National Laboratory, Los Alamos, New Mexico, USA

<sup>4</sup>Center for Integrated Nanotechnologies, Materials Physics and Applications Division, Los Alamos National Laboratory, Los Alamos, New Mexico, USA

<sup>5</sup>Archaeological Analysis and Graphics, Albuquerque, New Mexico, USA

<sup>6</sup>New Mexico State Historic Sites, Santa Fe, New Mexico, USA

## Correspondence

Brian M. Patterson, Engineered Materials Group, Materials Science and Technology Division, Los Alamos National Laboratory, Los Alamos, NM 87545, USA.  
Email: [bpatterson@lanl.gov](mailto:bpatterson@lanl.gov)

## Funding information

Los Alamos National Laboratory; U.S. Department of Energy's NNSA, Grant/Award Number: 89233218CNA000001

## Abstract

Two historic-period metal artifacts were provided by the New Mexico Historic Sites to Los Alamos National Laboratory for non-destructive analysis. The artifacts were a crossbow quarrel (or bolthead) and a reliquary pendant recovered from Kuaua Pueblo (also known as the Coronado Historic Site) in Bernalillo, NM. The quarrel is a heavily patinated metal that had been flattened due to compressive forces. The pendant consisted of a metal casing that had previously surrounded two center gemstones on the front and rear face of the pendant. The gemstone in the rear setting had fractured and was displaced from the setting, leaving only a small, loose fragment within the pendant for study. The front gem appeared to be very dark, near-black in color, and the fragment of the rear gem was a bright red color. The artifacts were analyzed to ascertain their composition and glean insight into their provenance using the following X-ray techniques: X-ray computed tomography, confocal micro X-ray fluorescence, and X-ray diffraction. Infrared spectroscopy and electron microscopy were used on selected areas. Ultraviolet Raman spectra were collected on the two gems and the pendant. The metal material of the artifacts was found to be primarily composed of copper. The gems in the pendant were composed of manganese (front gem) and calcium (side gem).

## KEYWORDS

artifacts, Coronado Historic Site, Kuaua Pueblo, New Mexico Historic Sites

## 1 | INTRODUCTION

Two metal artifacts were selected for analysis from a large assemblage of objects recovered from the Coronado Historic Site during a systematic near-surface metal detecting survey and a surface pedestrian survey undertaken by Dr. Clay Mathers between 2017 and 2021.<sup>1,2</sup> Both artifacts were found as part of a project to document a 1541 battle between elements of the Vázquez de Coronado expedition and the Southern Tiwa inhabitants of the Pueblo of Kuaua. The first artifact is a copper crossbow quarrel (or bolthead) (Figure 1a)—an object diagnostic of the Vázquez de Coronado expedition (i.e., *these weapons were outdated by the time later Spanish-led entradas reached New Mexico and the American Southwest*). The second artifact is a reliquary pendant (Figure 1b)—a very unusual Spanish Colonial object designed as a portable and personal receptacle for storing sacred/religious relics. This particular pendant may represent a votive charm, possibly employed as a talisman to protect

soldiers in battle or to offer spiritual and bodily protection for isolated Colonial landowners on the perilous edges of the empire. The composition of the metal appears to be a copper alloy, and it contains a black inset of mineral on one side and a fragment of a red mineral on the other. For this study, more details about the metal composition of this object are critical in determining whether it dates to the Early Colonial Period or belongs to a more modern era. If it is an Early Colonial artifact, it would be extremely important since no reliquary pendants are known yet from sixteenth-century contexts in North America.

Artifacts associated with the earliest expeditions (or *entradas*) in North America often have escaped the attention of generations of archeologists and historians.<sup>3</sup> Many of these objects were produced by a wide range of artisans and techniques in both the Old World and the Americas—including crossbow quarrels made by professional metal workers in Europe and Indigenous communities in Central and South America. These variations in



**FIGURE 1** Photographic images of the two artifacts.

(a) Crossbow quarrel (front-left, back-right). (b) Front and rear images of the pendant. (c) Side and bottom images of the pendant. The scale bar in (a) represents 4 cm and the scale bar in (b) and (c) represents 3 cm.

(Photographs courtesy of Clay Mathers). [Colour figure can be viewed at [wileyonlinelibrary.com](https://onlinelibrary.wiley.com/doi/10.1002/xrs.3330)]

metallurgical production, style, and “recipes,” made exotic forms of metal objects increasingly available, and sought after, worldwide as European expansion created an increasingly global network of exchange and communication. Unfortunately, the historical and archeological records have often been, until recently at least, somewhat mute about what types of objects were carried by early expeditions and what they looked like. To complicate matters further, archeologically derived objects that have been in the ground for approximately five centuries are often incomplete, damaged, oxidized, and corroded. Because of all these factors, identifying early historic metal objects can be challenging—especially when such attributions are based on visual inspection alone.

For this study, a variety of non-destructive techniques were used to understand the composition of two historic period metal artifacts from Kuaua Pueblo. All the following techniques allowed for a detailed study of both objects without requiring disassembly or destructive preparation techniques. The non-destructive nature of these analyses is important, since archeologists, museum curators, and others, are often reluctant to utilize any approaches that might alter or damage an object.

To examine the interior structures and material compositions of these artifacts, X-ray computed tomography (CT) was used. This is a powerful tool for visualizing the internal components and their arrangement. This instrument generates X-rays at a specified energy level and directs them toward a mounted sample. The mounted sample absorbs these photons based on the sample's density and composition. The X-rays that pass through the material are captured by the detector. X-rays are directed toward the sample from multiple orientations as the sample rotates. The measure of the decrease in X-ray intensity along this series of linear paths enables the reconstruction of tomographic images. These tomographic images can then be rendered into three dimensions, allowing for the inspection of all exterior and interior surfaces of the sample.

Confocal micro X-ray fluorescence can provide both single spectra and full spectral elemental maps. Elemental mapping displays the distribution of elements within the material. With polycapillary optics at both the excitation source and the detector, confocal X-ray fluorescence can spatially discriminate the source of the fluorescent X-ray photon in both the  $x$ - $y$  plane and the  $z$  direction. The ability to conduct compositional analysis of the pendant materials in their in situ environment (i.e., without requiring the removal of the gemstones from the pendant) makes XRF scanning an ideal technique for the study of this artifact. This technique uses a pair of

polycapillary optics to collect the fluorescent signal only from the gem and not from the underlying support.

X-ray diffraction (XRD) analysis is used to determine the atomic and molecular crystallographic structure of a material. A sample is irradiated with X-rays, and the subsequent intensities and scattering angle of the X-rays are measured, providing the average positions of atoms in the crystalline structure. XRD was used to determine if the material was crystalline, and if it was, what the phases were.

Fourier transform infrared (FT-IR) spectrophotometers measure specific wavelengths that cause a change in the dipole moments of sample molecules when the sample is exposed to infrared radiation. This raises the vibrational energy levels of the molecules to an excited state. Absorption peak intensity is related to the change in dipole moment and the possibility of energy level transitions.

UV-Raman spectroscopy was used to help complete our understanding of the spectral signatures of the gems and glean any information on their molecular fingerprints. Like the other techniques utilized here, it is non-destructive, and is therefore widely used to characterize materials of cultural provenance where in many cases it is necessary to excite materials at energies above those at which they fluoresce.

The scanning electron microscope equipped with energy dispersive spectroscopy (SEM-EDS) allows for composition-based contrast, which is especially helpful in the examination of multi-layer samples while collecting qualitative information about the elemental composition of regions of interest.

These techniques have been successfully employed in a variety of archeological investigations. X-ray CT has allowed for effective reconstructions of historical scrolls and manuscripts that have been heavily burned or subjected to excessive water damage with minimal manual manipulation of the objects. It also proved its value in the study and conservation of two water-saturated wooden objects from a 17th-century shipwreck.<sup>4</sup> XRF has aided in improving the understanding of historical changes in human-environment interactions related to obsidian procurement in central Japan during the Upper Paleolithic and provided insights into the pigment used in painted reliefs of fourth-century BC Etruscan tombs.<sup>5,6</sup> XRD, SEM-EDS, and FT-IR were effectively utilized together to study uncommon copper alloy artifacts dating back to the eighth-century BC and their complex degradation phenomena to develop strategies for long-term conservation.<sup>7</sup> Finally, Raman is widely used to study paintings, especially pigments, dyes, and paints and deep UV Raman is especially valuable to characterize geologic,<sup>8</sup> oxide,<sup>9</sup> and paleontological specimens.<sup>10</sup>



**FIGURE 2** X-ray CT image of the cross-bolt quarrel. Left—3D, surface thickness rendering, Right—YZ reconstructed slice. [Colour figure can be viewed at [wileyonlinelibrary.com](https://onlinelibrary.wiley.com)]

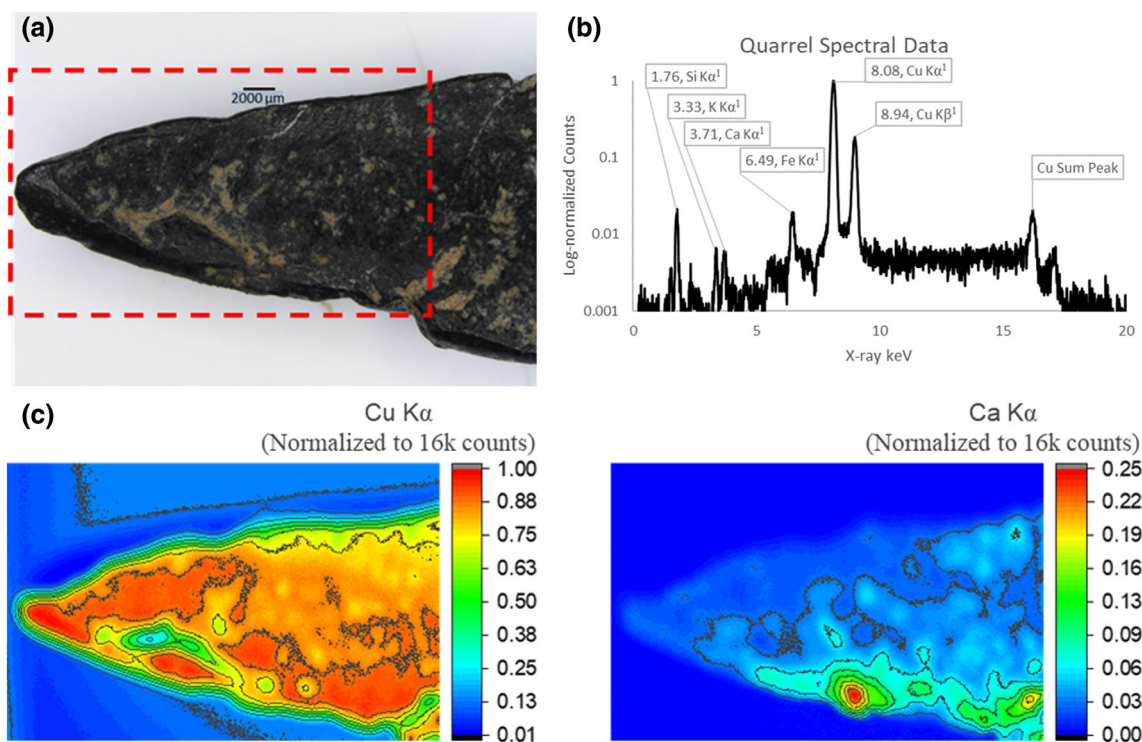
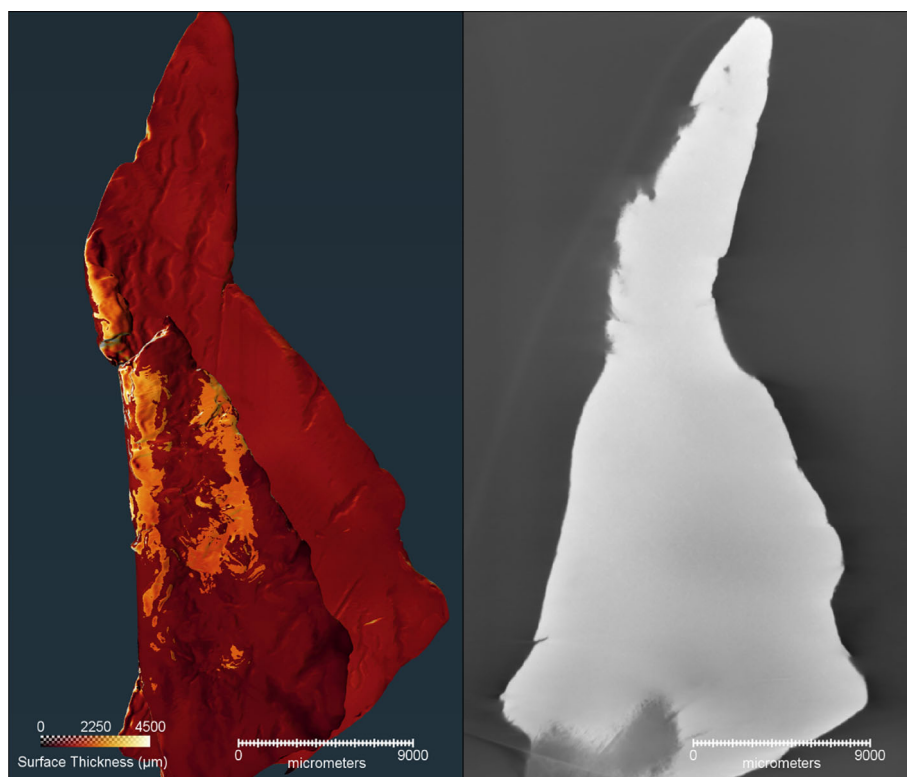


**FIGURE 3** (a) Image of analysis location (red box is the XRF mapped region), (b) spectrum of the crossbow quarrel, and (c) XRF maps for copper and calcium  $K\alpha$  signals. [Colour figure can be viewed at [wileyonlinelibrary.com](https://onlinelibrary.wiley.com)]

## 2 | EXPERIMENTAL

### 2.1 | X-ray computed tomography

A Carl Zeiss X-ray Microscopy Inc. Xradia 520 Versa (Pleasanton, CA) was used for imaging the cross-bow quarrel. A total of 3201 images of the quarrel were collected at 160 (peak kilovolts) kVp and 10 watts (W) with an exposure time of 4.823 s using the 0.4 $\times$  objective and HE 18 filter with a binning of 2, resulting in a 26.12 micrometer ( $\mu$ m) voxel size. A North Star Imaging X5000 (Rogers, MN) was used to image the pendant. This instrument was needed due to the lead used to hold the pendant together. A total of 740 projections of the pendant were collected at 450 kVp and 1500 microamperes ( $\mu$ A) with a 1 s exposure time using a flat panel detector and 0.25 mm Cu filter. The panel pixel pitch was 100  $\mu$ m magnified by 1.25 and then a sub-pixelation was performed to produce an effective voxel size of 40  $\mu$ m.

### 2.2 | Confocal micro X-ray fluorescence

A custom-built confocal micro X-ray fluorescence instrument was used in both 2D and 3D modality. 2D elemental maps were conducted on both artifacts. A 7  $\times$  12 mm section around the tip of the quarrel was imaged in 30  $\mu$ m steps at 20.0 kV and 0.8 mA with a dwell time at each location of 3 s and a peaking time of 5  $\mu$ s. The map was 233.33  $\times$  400 pixels and required 177 h to collect. A 9.75  $\times$  10 mm section around the upper right corner of the central gemstone and the associated case was imaged in 100  $\mu$ m steps at 25.0 kV and 0.5 mA with a dwell time of 3 s and peaking time of 5  $\mu$ s. The map was 97.5  $\times$  100 pixels and required 16 h to collect. Confocal spectra were obtained from the center gemstone and side gemstone. These measurements were obtained at 30.0 kV and 0.5 mA with a dwell time of 120 s and peaking times of 60  $\mu$ s (side gemstone) and 40  $\mu$ s (center gemstone).

### 2.3 | X-ray diffraction

XRD was performed to determine the phases present in the supplied artifacts. XRD measurements were performed on a Bruker AXS D8 Advance system (Madison, WI) with a Cu K $\alpha$  source using locked couple  $\theta$ -2 $\theta$  scans, diffraction intensity was collected in 1D mode using a Lynxeye-XET position sensitive detector. The measurement data presented in the following figures are shown with XRD intensity on the y-axis (counts) and 2 $\theta$  (degrees) on the x-axis. Also shown are peak positions from powder diffraction files (PDF) for phases of

importance to this study which were obtained from the International Centre for Diffraction Data (ICDD<sup>®</sup> 2021) database. Mainly, if the intensities from the database peaks index (align) with the sample XRD pattern peaks, it indicates that this phase is present in the sample. Slight deviations between the database PDF peak positions arise from differences in lattice parameters due to stoichiometry. Nonetheless, the comparison of the PDF patterns with the measured patterns is strictly for determining the existence of the phases in the supplied artifacts and not the exact chemistry.

### 2.4 | Raman spectroscopy

Deep UV Raman spectra were collected at multiple locations on each of the gems and the pendant metal. Raman spectroscopic measurements were conducted in ambient conditions in reflection mode using 244.0 nm (5.081 eV) continuous wave excitation at 10 mW output (Cambridge Laser Laboratories LEXEL Quantum 8 SHG continuous wave tunable Argon ion laser), in a Horiba LabRAM HR Evolution high-resolution confocal Raman microscope (Pasadena, TX). The experiment was configured using a 2400 mm<sup>-1</sup> holographic grating blazed at 250 nm, a 50  $\mu$ m confocal hole diameter, and a 74 $\times$ , 0.65 N.A. reflective objective. Spectral calibration was performed using the 1332.5 cm<sup>-1</sup> band<sup>11</sup> of a synthetic Type IIa diamond, and spectral intensity was calibrated using a VIS-halogen light source (NIST test no. 685/289682-17). Instrumental linewidth broadening was measured using a Hg(Ar) spectral calibration lamp (Oriel 6035) to be  $\sim$ 3.2 cm<sup>-1</sup> in the configuration used here.

### 2.5 | Other instrumentation

Additionally, a Thermo-Fisher Scientific Nicolet iS50R FT-IR (Waltham, MA) collected a spectrum on the black mineral on the pendant and an EDS map was collected on the crossbow quarrel using a JEOL Ltd. JSM-IT100 SEM operating at 20.0 kV.

## 3 | CROSSBOW QUARREL RESULTS AND DISCUSSION

X-ray CT of the crossbow quarrel revealed little variation in the density of the material (Figure 2). The 2D XRF scan of the quarrel tip (Figure 3) shows the major compositional element to be copper, with only trace amounts of silicon, potassium, calcium, and iron, likely from soil contamination as the samples were not cleaned.

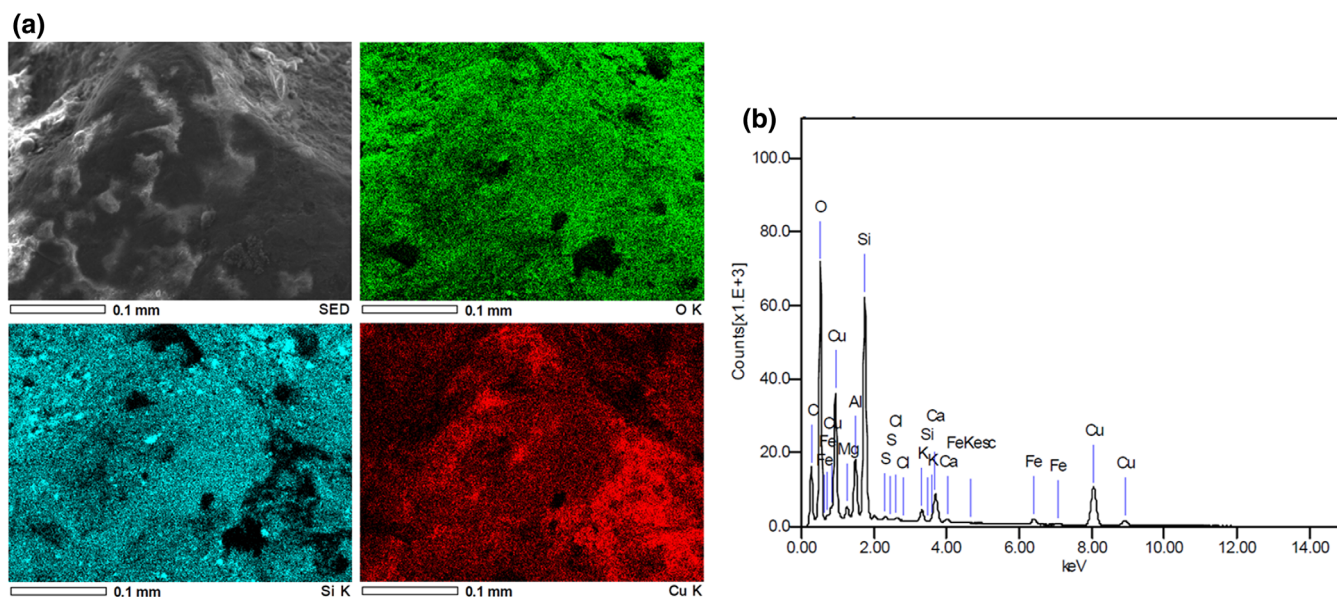


**FIGURE 4** (a) SEM image and EDS map of the crossbow quarrel with composite spectrum. The top left is the secondary electron image and clockwise; oxygen, copper, and silicon elemental maps. (b) Composite spectrum of the quarrel. [Colour figure can be viewed at [wileyonlinelibrary.com](http://wileyonlinelibrary.com)]

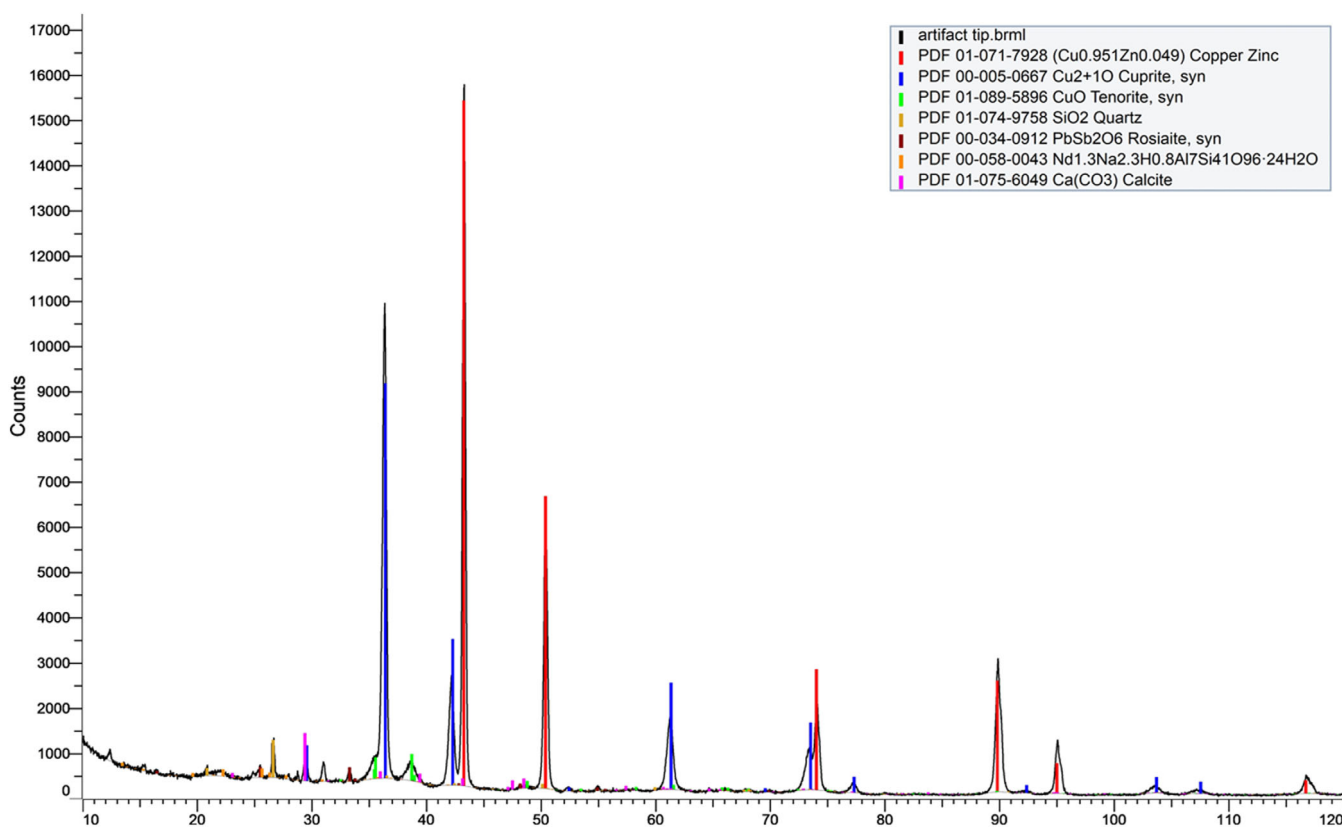


**FIGURE 5** XRD pattern of the crossbow quarrel. [Colour figure can be viewed at [wileyonlinelibrary.com](http://wileyonlinelibrary.com)]

Significantly, these results are consistent with XRF and pXRF analyses carried out on other Vázquez de Coronado materials from Kuaua and Pecos Pueblo in New Mexico, and on objects linked with the early expeditions

of Hernando de Soto (1539–1543) and Tristán de Luna y Arellano (1559–1561) in what is now the southeastern United States.<sup>3,12,13</sup> Since this scan was performed at a constant *z*-height above the sample, some of the variation



in signal intensity seen in Figure 3 can be attributed to variations in the surface profile of the quarrel. The SEM/EDS instrument struggled to penetrate beyond the oxide and soil contamination layers to analyze the material underneath. The most prominent signals were silicon and oxygen, followed by copper with trace amounts of other elements. Figure 4a shows the area imaged by EDS and the maps for O, Si, and Cu. Spectral results are provided in Figure 4b. The strongest signals in the XRD analysis of the quarrel (Figure 5) were copper-zinc alloy and cuprite, an oxide mineral of copper. The other mineral-type phases present are likely due to soil interactions with the artifact during aging. The uniformity of

material composition throughout the specimen, coupled with the results of XRF and XRD would indicate that copper is the primary elemental composition of this material.

High-resolution results of the type reported here are important for several reasons. First, crossbow quarrels—both copper and iron—are known to be associated with the earliest Spanish-led expeditions in North America, dating from the beginning of the sixteenth century to about the early 1570s. In what is now New Mexico and the Greater American southwest, crossbows and quarrels are absent from all of the later sixteenth-century entradas that followed the Vázquez de Coronado expedition—that is,

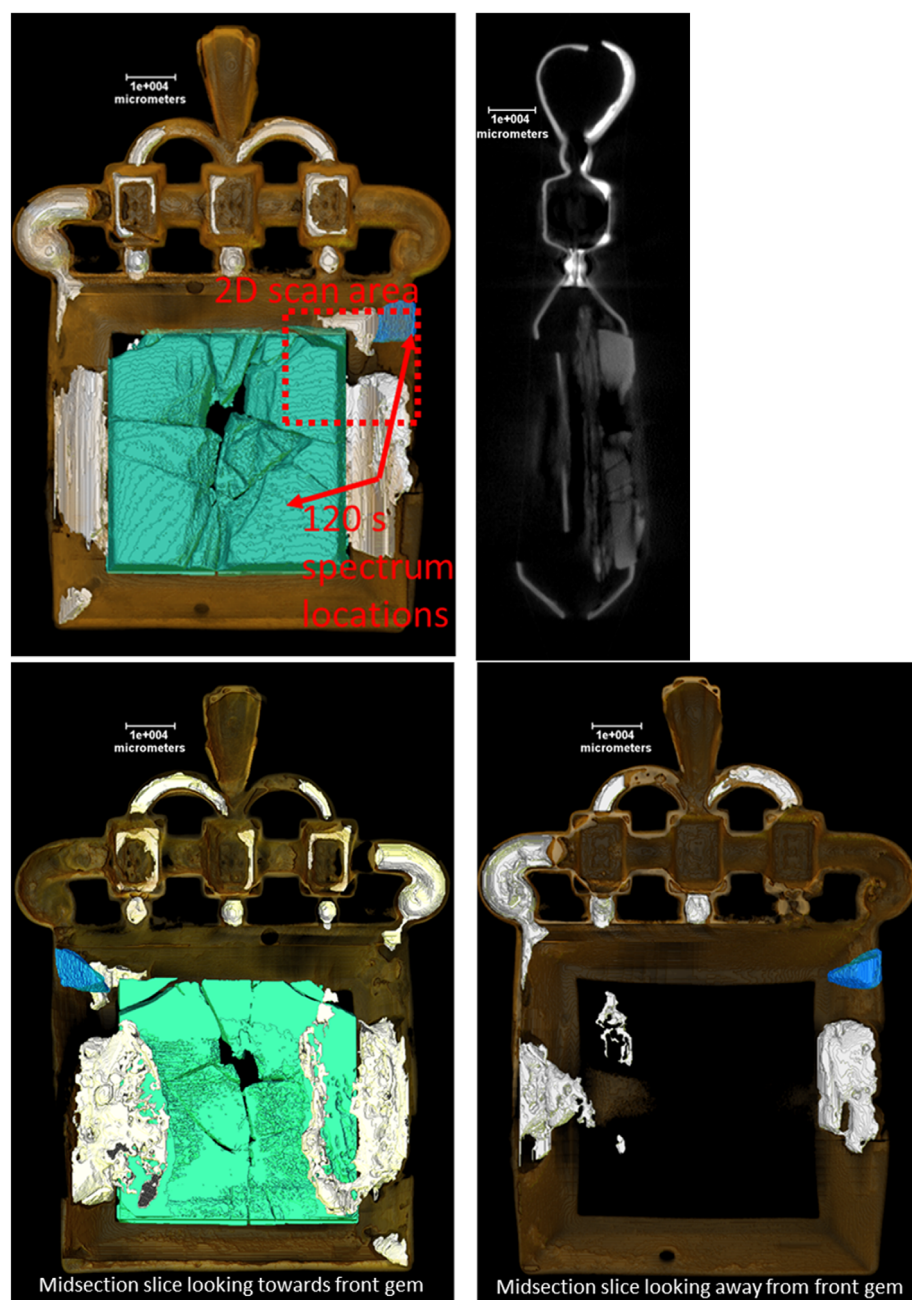
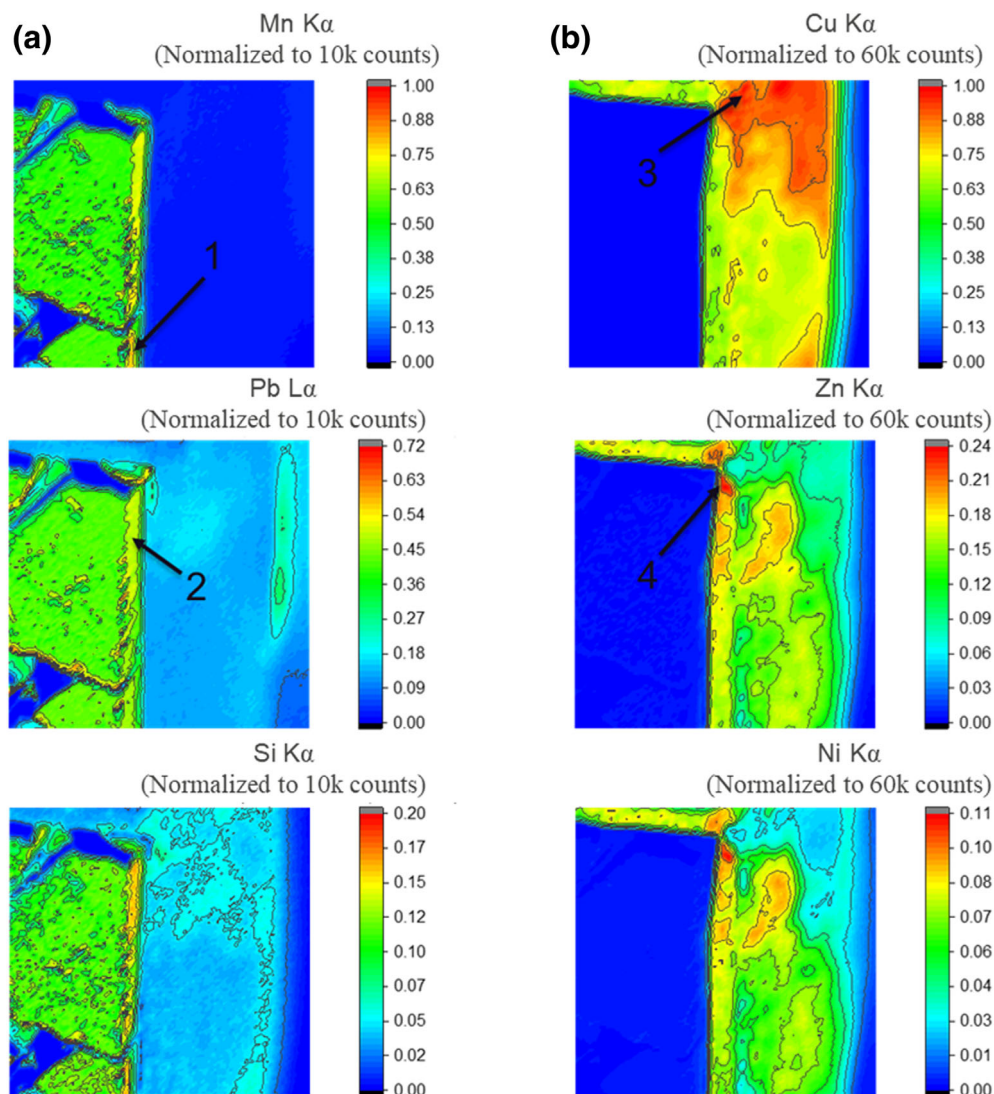


**FIGURE 6** 3D X-ray CT renderings and reconstructed XZ orthogonal slice of the pendant. Upper left image indicates the locations of XRF analyses. Green—center gemstone, cream—bonding agent, and blue—side gemstone. [Colour figure can be viewed at [wileyonlinelibrary.com](https://onlinelibrary.wiley.com/doi/10.1002/xrs.3330)]

**FIGURE 7** 2D XRF maps of the upper right portion of the pendant (shown in Figure 6). Column (a) highlights elements composing the center gemstone and column (b) indicates those that make up the casing. Numbered arrows indicate locations chosen for spectral analysis in Figure 8. [Colour figure can be viewed at [wileyonlinelibrary.com](https://onlinelibrary.wiley.com)]



from 1543 to the end of the sixteenth century. Second, because crossbow quarrels are such a securely dated and diagnostic artifact details regarding its composition provide an important baseline for evaluating other suspected early objects—including more incomplete and ambiguous fragments belonging to crossbow quarrels and other cupreous artifacts. Comparisons of these data with XRF analyses from other suspected entrada sites and objects may, therefore, produce valuable insights. Finally, these results may help us to better evaluate the historical development of metallurgy in New Spain, as new technologies and resources were developed and exploited, and as Old and New World traditions began to merge with one another.

#### 4 | PENDANT RESULTS AND DISCUSSION

X-ray CT of the pendant found four distinct components; the center black gemstone, the casing, a fragment of the

potential rear red gemstone (lodged in the casing along the side, referred to as side gemstone), and a high- $z$  material used as a bonding agent. This bonding agent appeared to hold the center black gemstone in place, as well as adhere the case halves together. The high density of the bonding agent produced imaging artifacts that limited the ability to obtain the completion of the material segmentation.

The 2D XRF map and confocal results indicate that the primary constituents of the center gemstone were manganese and lead, along with smaller amounts of silicon and potassium (Figure 7a, b). The 2D scan also indicates a lead presence in the area where the side gemstone was slightly protruding from the edge of the case, shown in the middle image of Figure 7a. In this instance, it is difficult to determine if the side gem contained lead, or if this result contributed to surface contamination from brushing against the internal bonding material, which contains lead. The casing of the pendant was predominately comprised of copper, with lesser amounts of zinc, nickel, calcium, and



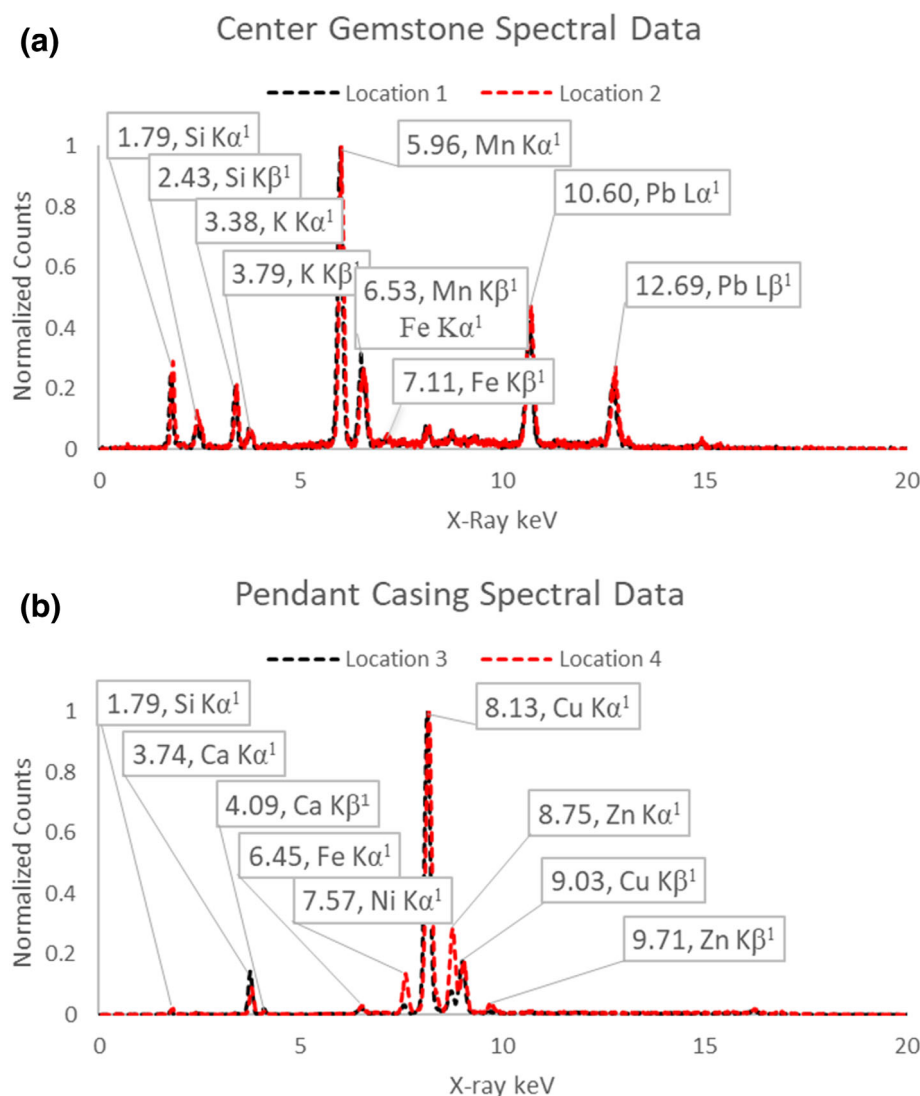


FIGURE 8 Spectral data obtained from gemstone (a) and casing (b) analysis locations correspond to marked positions in Figure 7. [Colour figure can be viewed at [wileyonlinelibrary.com](https://onlinelibrary.wiley.com/doi/10.1002/xrs.3330)]

iron (Figures 7, 8). The confocal spectrum of the center gemstone (Figure 9a) confirms the results from the 2D scan with consistent elemental composition and the confocal spectrum of the side gemstone (Figure 9b) reveals a predominate calcium composition, with lead and silicon, as well as trace amounts of potassium and iron.

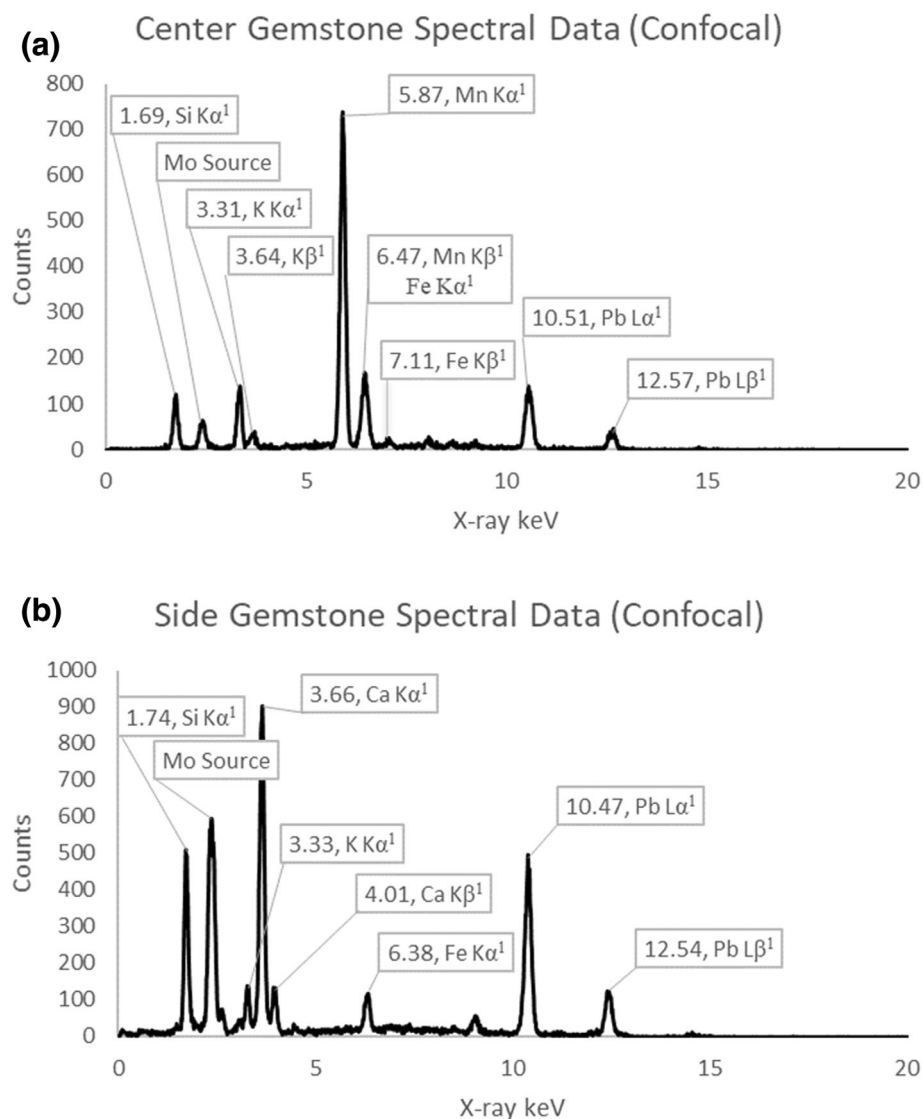
XRD results on the pendant case (Figure 10) show a strong presence of Cu–Zn like phases, along with Cu–O phases and a mineral-type calcite phase present as a relatively thick surface layer. The prominent Raman spectrum with bands at 716, 1089, 1440, and 1751 index as calcite  $\text{CaCO}_3$ , confirms its presence. These Raman peaks also show up in the black gem (Figure 11). This calcite layer was most likely due to soil interactions with the artifact during aging. This layer was notably thicker than the surface layer present on the crossbow quarrel, indicated by the higher intensity signals in the quarrel analysis.

The results on the black center gemstone (Figure 12) indicate that the center gemstone does not contain a

crystalline mineral, as it exhibits a classic amorphous XRD pattern. Potter and Rossman explain that the use of XRD for the mineralogy of manganese oxides is difficult due to their fine-grained, poorly crystalline structure.<sup>14</sup> Their study recommends the use of infrared spectroscopy (IR) to assist with analysis. XRD analysis of the side gemstone was unable to determine the phase after several attempts. Due to time constraints, the team was unable to modify a holder that would allow for a strong diffraction signal. Ideally to get the best signal, the stone would have to be removed for XRD measurements, in contrast with our non-destructive analytical approach. Raman spectroscopy (Figure 11a) of the red gem indicates that it may come from  $\text{Ca}(\text{Fe}, \text{Mg}, \text{Mn})(\text{CO}_3)_2$  alloy carbonate. Raman spectroscopy of the black gem indicates a possible transition metal-doped alumina glass (Figure 11b, c).

The IR spectrum of the black center gemstone (Figure 13) has peaks at wavenumbers 973.4, 767.1, and  $429.1 \text{ cm}^{-1}$ . The Potter publication presents several

**FIGURE 9** Confocal XRF spectral data for (a) center gemstone and (b) side gemstone. Locations of analysis are annotated in Figure 7.



manganese oxide mineral species containing two to three peaks; around  $1000\text{ cm}^{-1}$ , in the  $800\text{--}600\text{ cm}^{-1}$  range, and  $500\text{--}400\text{ cm}^{-1}$  range. Another important observation is the lack of organic signatures in this spectrum. The absence of carbon bonds allows for the elimination of jet (lignite) as a candidate for the center gemstone.

The results of these analyses confirm that the primary elemental constituent of the metals in the quarrel and pendant is copper. The pendant casing elemental analysis suggests that this metal is an alloy containing copper, zinc, and nickel. It is believed that the trace amounts of silicon and iron are potentially soil contamination. Calcium is used as an alloying agent and helps deoxidize copper without any material impairment to its mechanical properties. Small amounts of calcium have been used to increase copper's resistance to embrittlement. The compositional materials of copper, zinc, and nickel may have significance in the history of origin for this pendant.

In a submission to the Committee on Asiatic Studies in American Education, Dr. Derk Bodde explains that this alloy, commonly referred to today as German silver, was not mentioned in European references until 1597, when it began arriving via Chinese trade routes as a metal called paktong (pai tongs), which means white copper in Cantonese.<sup>15</sup> Paktong was entirely imported from Asia until about 1750, when German metallurgists began producing imitation material. Importation came to a halt in the 1830s once the manufacturing methods for this compound metal were introduced to industrialized England, and paktong lost its original name.<sup>16,17</sup>

Despite these data, a definitive chronology for this pendant is not yet possible. Nevertheless, the detailed compositional information derived from these analyses will be helpful in addressing possible stylistic and metallurgical parallels with professional colleagues in the Americas, Europe, and elsewhere. Counterfeit jewelry

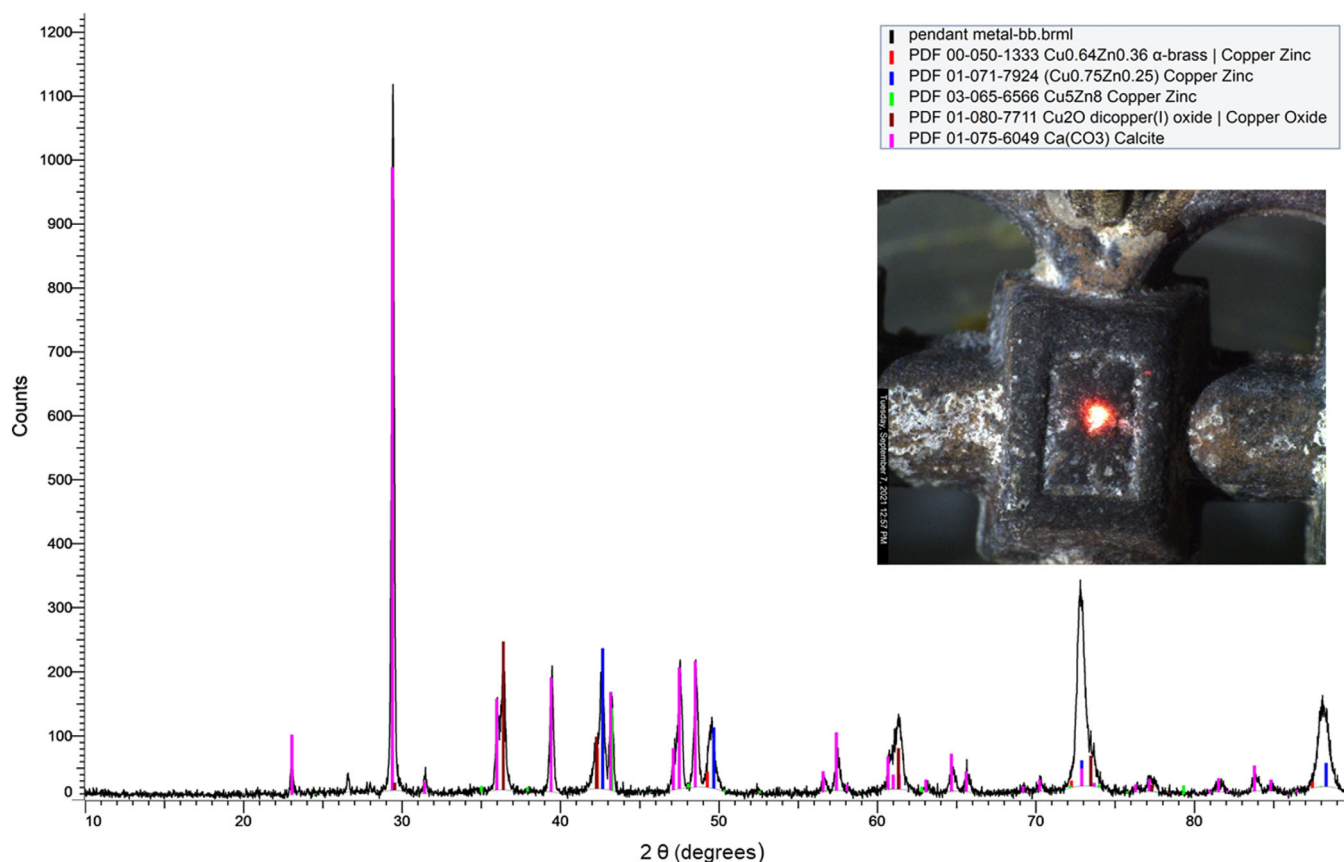


FIGURE 10 XRD of pendant case. [Colour figure can be viewed at [wileyonlinelibrary.com](https://onlinelibrary.wiley.com/doi/10.1002/xrs.3330)]

was especially commonplace in sixteenth- and seventeenth-century Europe,<sup>18</sup> as was the use of semi-precious black and red gemstones and other materials as charms or talismans (such as jet and coral or garnet, respectively).<sup>19,20</sup> A wide variety of copper alloys were also used commonly in the Late Medieval and Early Modern periods for jewelry and other personal ornaments.<sup>21</sup> Further investigation of the stylistic and elemental attributes of this complex object will continue. In the meantime, we hope that the approaches outlined in this discussion will assist other scholars in addressing their own challenges in identifying definitive dates and origins for their historical artifacts.

The center gemstone is an amorphous material that lacks a crystalline structure. The minor contribution of silicon in the material coupled with the findings that manganese oxide is fine-grained with poor crystallinity. The lack of organic signatures in the FT-IR spectrum also eliminates jet as a potential candidate. XRF was successful in detecting elements at the surface of the material, finding calcium, silicon, lead, potassium, and iron. The elemental composition and the amorphous composition indicate that the gem could be glass, but

the absence of red color producing elements like manganese, selenium, or copper-tin from the spectrum make a definitive identification difficult. Further conclusions on the side red gem will not be possible without further analysis.

## 5 | CONCLUSIONS

The battery of non-destructive analyses performed on two metal artifacts from Kuaua Pueblo (Coronado Historic Site) illuminated several interesting details about these materials. X-ray CT analysis revealed interior surfaces and materials within the pendant, indicating the locations of the remaining bonding material inside. XRF and XRD allowed for qualitative elemental composition and structural order analysis of both artifacts, indicating that both the quarrel and pendant metals were predominately copper, with the pendant being shown to consist of a copper alloy. XRF results of the center gemstone indicated that manganese and lead were the prominent constituents, but it was difficult to obtain definitive data from the side gemstone fragment due to its positioning

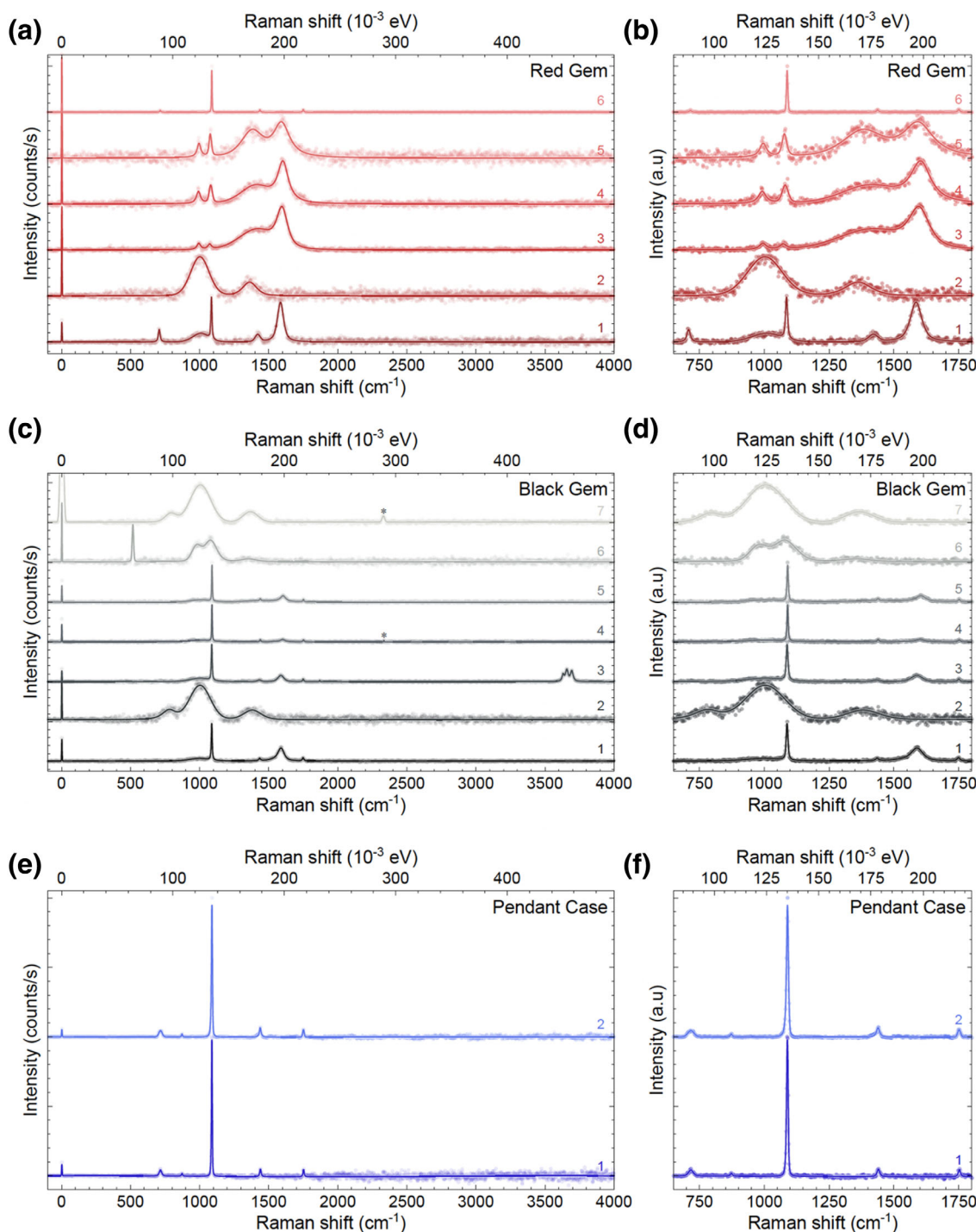


**FIGURE 11** Raman spectra of the (a, b) red gemstone, (c, d) black gemstone, and (e, f) pendant case taken at different locations using 244 nm laser excitation. Data are shown after background removal (circles) and fitting with Lorentzian peaks (solid lines), where left panels present wide spectral window scans and right panels present the region between 650 and 1800  $\text{cm}^{-1}$ . Atmospheric nitrogen is indicated by the asterisks. [Colour figure can be viewed at [wileyonlinelibrary.com](https://onlinelibrary.wiley.com/terms-and-conditions)] [wileyonlinelibrary.com](https://onlinelibrary.wiley.com/terms-and-conditions)]

mobility within the pendant. XRD revealed that the center gemstone lacked any crystalline structure, and the FT-IR results presented an absence of organic material in its composition. XRD and SEM-EDS confirmed the presence of soil contamination and oxide layers on the

surfaces of both the quarrel and pendant. More detailed quantification of the metals on the quarrel and pendant may be obtained by etching a small area to remove the oxide layer and aging interaction layer to solely measure the base material.



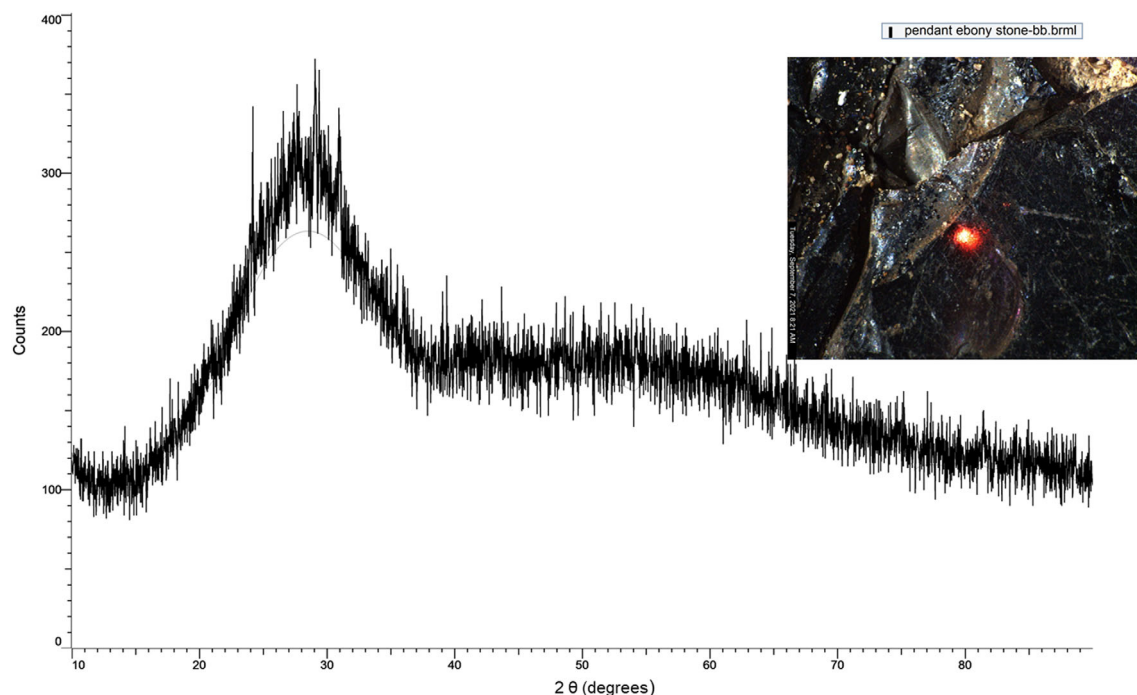


**FIGURE 12** XRD of the center gemstone, the broad peak and lack of narrow bands indicate that the material is amorphous in structure. [Colour figure can be viewed at [wileyonlinelibrary.com](http://wileyonlinelibrary.com)]

#### IR Spectrum of Center Gemstone

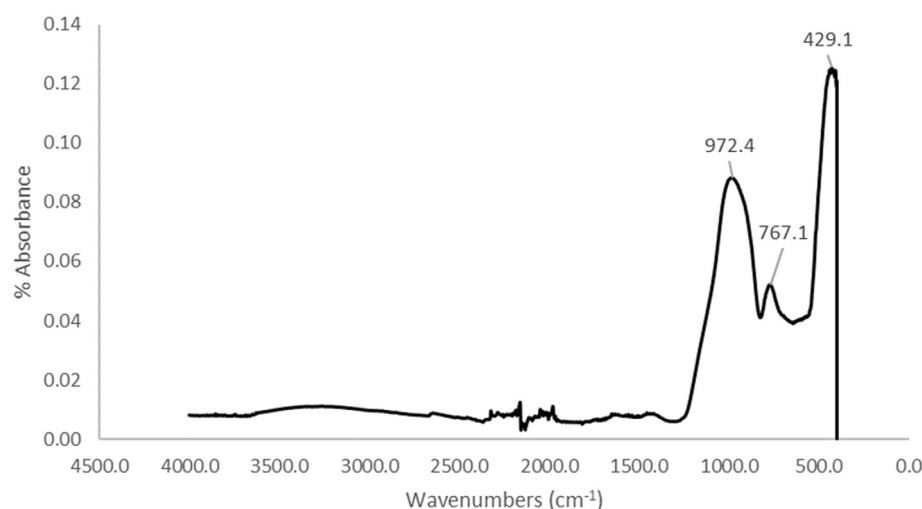


**FIGURE 13** FT-IR spectrum of the black gem.

#### ACKNOWLEDGEMENTS

Funding for this project was provided by the Community Partnership Office via outreach specialist, Patrick Duran. We would also like to thank the Register for Professional Archeologists and the Friends of the Coronado Historic Site for their generous funding for pXRF testing of archeological metal objects from the Kuaua Environs Survey, and the following scholars for their insights regarding the identification and possibly chronology of the reliquary pendant (i.e., Professor Charles Cobb and Dr. Gifford

Waters [Florida Museum of Natural History] and Dr. Jorge Rivas Pérez [Denver Art Museum]. This work was performed, in part, at the Center for Integrated Nanotechnologies, an Office of Science User Facility operated by the U.S. Department of Energy (DOE) Office of Science. Los Alamos National Laboratory, an affirmative action equal opportunity employer, is managed by Triad National Security, LLC for the U.S. Department of Energy's NNSA, under contract 89233218CNA000001. LA-UR: 23-21163.




## DATA AVAILABILITY STATEMENT

The data that support the findings of this study are available from the corresponding author upon reasonable request.

## ORCID

Alex Edgar  <https://orcid.org/0000-0002-9719-3683>

Brian M. Patterson  <https://orcid.org/0000-0001-9244-7376>

## REFERENCES

- [1] C. Mathers, *Pap. Archaeol. Soc. New Mexico* **2020**, 46, 175.
- [2] C. Mathers, *Pap. Archaeol. Soc. New Mexico* **2021**, 47, 101.
- [3] C. Mathers, *The Destiny of Their Manifests: Entrada Assemblages and the Challenge and Promise of Modeling Deep History*, Sixteenth-Century Assemblages in North America, Modeling Entradas **2020**, p. 1.
- [4] K. E. Rankin, Z. J. Hazell, A. M. Middleton, M. N. Mavrogordato, *J. Archaeol. Sci. Rep.* **2021**, 39, 103158.
- [5] Y. Suda, T. Adachi, K. Shimada, Y. Osanai, *J. Archaeol. Sci.* **2021**, 129, 105377.
- [6] M. Alfeld, C. Baraldi, M. C. Gamberini, P. Walter, *X-Ray Spectrom.* **2019**, 48(4), 262.
- [7] G. M. Ingo, C. Riccucci, C. Giuliani, A. Faustoferri, I. Pierigè, G. Fierro, M. Pascucci, M. Albini, G. di Carlo, *Appl. Surf. Sci.* **2019**, 470, 74.
- [8] A. C. Strzelecki, S. Chariton, C. B. Cockreham, M. T. Pettes, V. Prakapenka, B. A. Chidester, D. Wu, C. R. Bradley, G. G. Euler, X. Guo, H. Boukhalfa, H. Xu, *Phys. Chem. Miner.* **2022**, 49(12), 45.
- [9] Y. Sharma, B. Paudel, A. Huon, M. M. Schneider, P. Roy, Z. Corey, R. Schönemann, A. C. Jones, M. Jaime, D. A. Yarotski, T. Charlton, M. R. Fitzsimmons, Q. Jia, M. T. Pettes, P. Yang, A. Chen, *Adv. Sci.* **2022**, 9(33), 2203473.
- [10] J. Alleon, G. Montagnac, B. Reynard, T. Brulé, M. Thoury, P. Gueriau, *BioEssays* **2021**, early view(n/a), 43, 2000295.
- [11] S. A. Solin, A. K. Ramdas, *Phys. Rev. B* **1970**, 1(4), 1687.
- [12] D. D. Scott, P. Bleed, C. Haecker, *The Pecos Trade Fair Area: Archeological Investigations of Apache, Comanche, and Spanish-Related Sites at Pecos National Historic Park, New Mexico*, I.R. National Park Service, Santa Fe, New Mexico, Editor. **2014**.
- [13] S. E. Linden, *Materials of Conquest: A Study Using Portable X-ray Fluorescence Spectrometry in the Metallurgical Analysis of Two Sixteenth Century Spanish Expeditions*, University of West Florida, Tallahassee **2013**.
- [14] R. M. Potter, G. R. Rossman, *Am. Mineral.* **1979**, 64(11–12), 1219.
- [15] D. Bodde, *China's Gifts to the West* (Ed: C. University), Columbia University, New York City, **2004**, p. 1.
- [16] F. D. Jones, E. Oberg, *Machinery's Encyclopedia; A Work of Reference Covering Practical Mathematics and Mechanics, Machine Design, Machine Construction and Operation, Electrical, Gas, Hydraulic, and Steam Power Machinery, Metallurgy, and Kindred Subjects in the Engineering Field*, The Industrial Press, New York **1917** [etc., etc.]. 7 v.
- [17] C. L. Mantell, C. Hardy, *Trans. Electrochem. Soc.* **1934**, 66(1), 63.
- [18] A. Mottana, *J. Gemmol.* **2017**, 35(7), 652.
- [19] R.A. Johnson, *All Things Medieval: An Encyclopedia of the Medieval World*, ABC-CLIO, LLC, Santa Barbara **2011**.
- [20] M. A. Hall, *J. Mater. Cult.* **2011**, 16(1), 80.
- [21] G. Egan, F. Pritchard (Editors), *Dress Accessories c. 1150-c. 1450. Medieval Finds from London 3*. Museum of London, London **2002**.

**How to cite this article:** S. G. Young, J. Valdez, M. Espy, A. Edgar, J. Brett, M. T. Pettes, C. Mathers, M. Barbour, B. M. Patterson, *X-Ray Spectrom* **2024**, 53(1), 2. <https://doi.org/10.1002/xrs.3350>